CHAPTER IV

MINERALOGY OF BALL CLAYS AND THEIR ORIGIN

In general, a ball clay is a fine-grained sedimentary deposit composed essentially of kaolinite of approximately 50 to 90 per cent. The other minerals are quartz, micas, and illite or hydrous mica. As with all sedimentary deposits, ball clays may contain small amount of rutile, anatase, montmorillonite, carbonaceous matter, and other fine-grained mineral fragments. The total iron oxide content usually does not exceed 2.5 per cent. The small particle size, with approximately 80 per cent smaller than one micron, and high clay mineral content of these deposits cause them to be highly plastic and exhibit great drying shrinkage. The geometry of ball clay deposits, in general, are lenticular and they are in most cases of lacustrine origin.

In the previous chapters, the detailed geology, sedimentary sequences and their distribution in the Mae Than basin have been described. In this chapter, the detailed clay mineralogy of some selected claystones and the commercial "ball clay", including the possible origin of ball clay will be discussed.

Claystones from 5 drill-holes were used for characterization for their detailed clay mineral constituents by the X-ray diffractometry technique combined with ethylene glycolation, and heat treatment at 550°C (Harry et al. 1984). The commercial ball clays (claystones of Unit B) from the Banpu mine pit and 4 selected claystones from 2 drill-holes (Unit A and F from the drill-hole nos. MT-14 and MT-15) were also identified by the differential thermal and thermo-gravimetric analyses (DTA/TG), and the crystal habits were also observed under the scanning electron microscope (SEM) with attached EDS.

Representative examples of qualitative XRD analysis of a commercial "ball clay" (Unit B) and a claystone of Unit D are illustrated in Figures 4.1 and 4.2. These

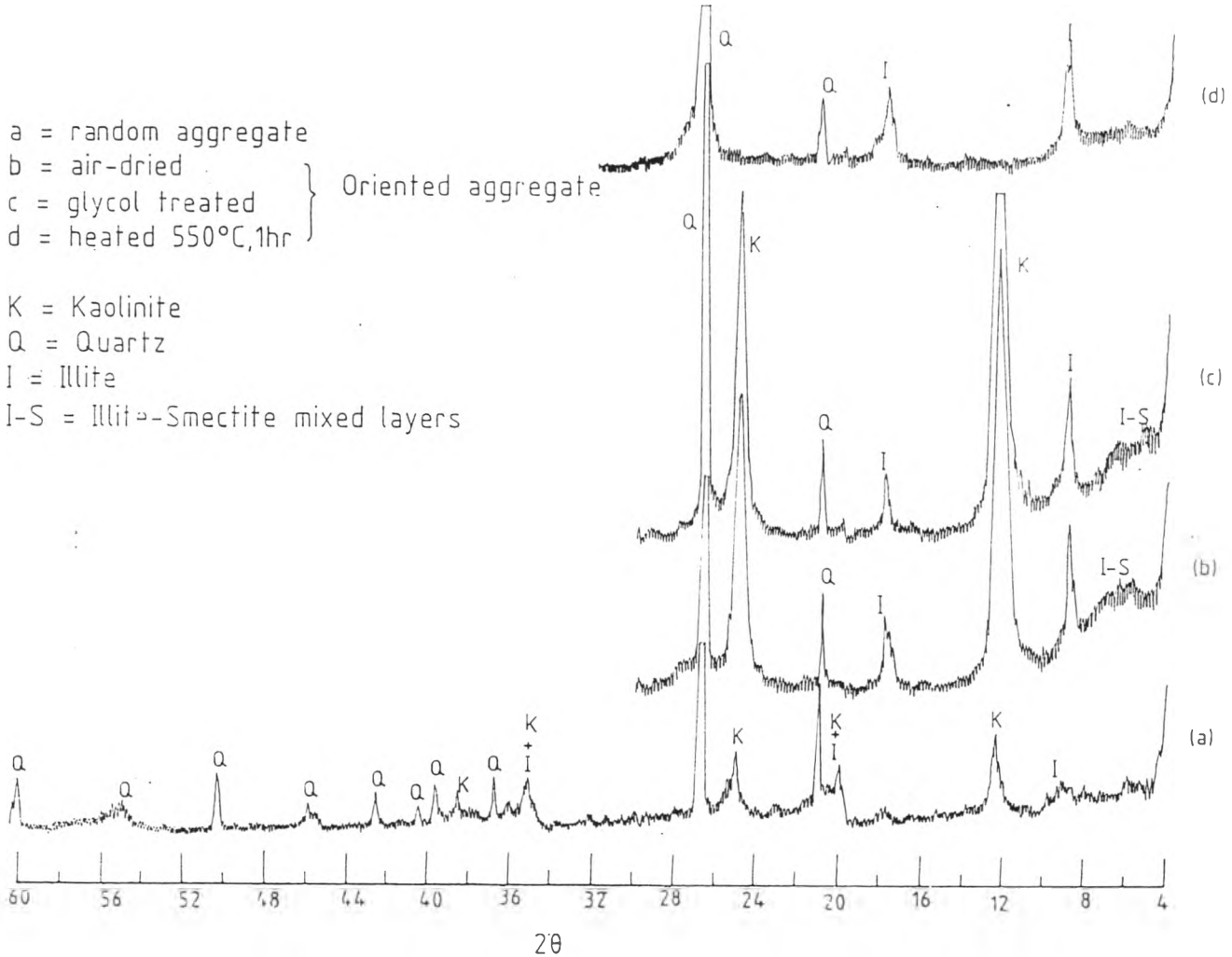

Fig. 4.1 X-ray diffractograms of claystone (Unit B) from the Mae Than basin.

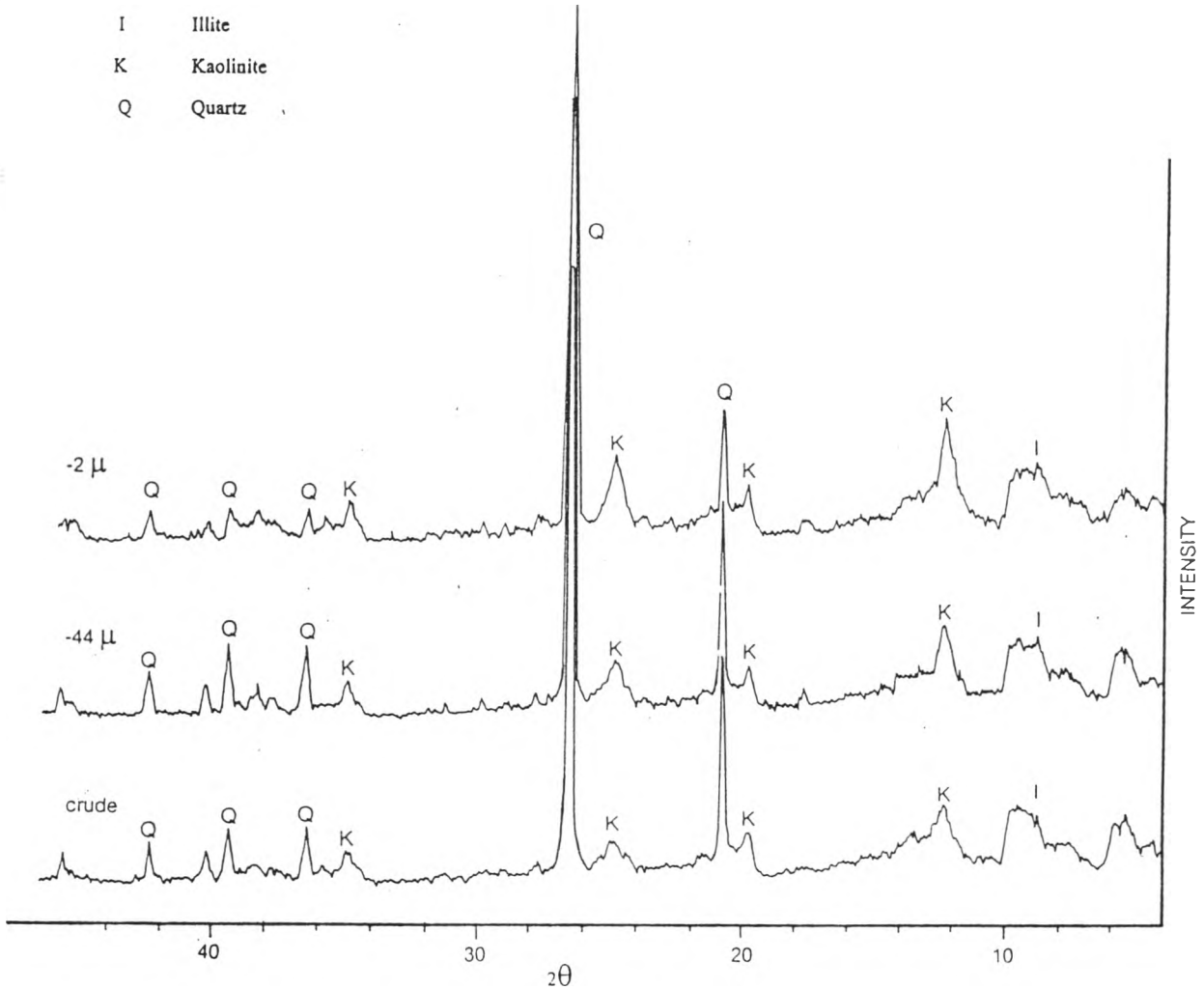

Fig. 4.2 X-ray diffractograms of various particles size fractions of claystone (Unit D) from the Mae Than basin.

data (together with those in Figure 4.3) reveal that most of the claystones including the commercial "ball clay" comprise of a mixture of kaolinite, illite, and quartz as the major constituents. The smectite or illite-smectite mixed-layer clays occasionally occur as only a trace constituent (normally less than 5 per cent). The XRD analysis reveals that quartz is the major component in the sand and silt fractions, whereas kaolinite and illite as expected are the major constituents in the clay fractions (Fig. 4.3).

The DTA/TG analyses of the clay fractions of a commercial "ball clay", notably, the claystones from Unit A, Unit D and Unit F from 2 drill-holes, MT-14 and MT-15, are presented in Figures 4.4 to 4.7. The DTA/TG data reveal the characteristic peaks of kaolinite. The main endothermic dehydroxylation peaks of the kaolinite are slightly asymmetric and occur at approximately 570°C for all the samples. The exothermic peaks, due to the formation of mullite, appear at the temperature range of 978°C to 1,000°C. The asymmetric nature and dehydroxylation temperatures suggested that the kaolinite group mineral is a poorly crystallized kaolinite and/or halloysite rather than dickite or nacrite which commonly give the symmetrically endothermic dehydroxylation peak at around 700°C (Brindley and Porter, 1978; Mackenzie, 1975). The crystal habit (see SEM data in the next paragraph) reveals that this kaolinite group mineral is a platy pseudo-hexagonal kaolinite rather than tabular halloysite. The small endothermic peaks appeared at 70°C to 123°C are mainly due to the loss of adsorbed water. It should be noted that the main endothermic and exothermic peak temperatures of the kaolinite in the claystones from the Mae Than basin are exactly the same as those (i.e., endothermic peak temperature at 566°C and exothermic peak temperature at 996°C) observed in the weathered rhyolitic tuff found on the western margin of the basin. This may indicate their common origin.

The scanning electron micrographs of crude claystones from the Banpu mine pit of Units B and D show the random aggregates of platy kaolinite and illite without tabular halloysite (Figs. 4.8 to 4.18). No vermiform kaolinite or stack of illite (indicative of *in situ* formation) has been detected. They rather represent an aggregate of individual plates of kaolinite and illite which many of them show a broken outline.

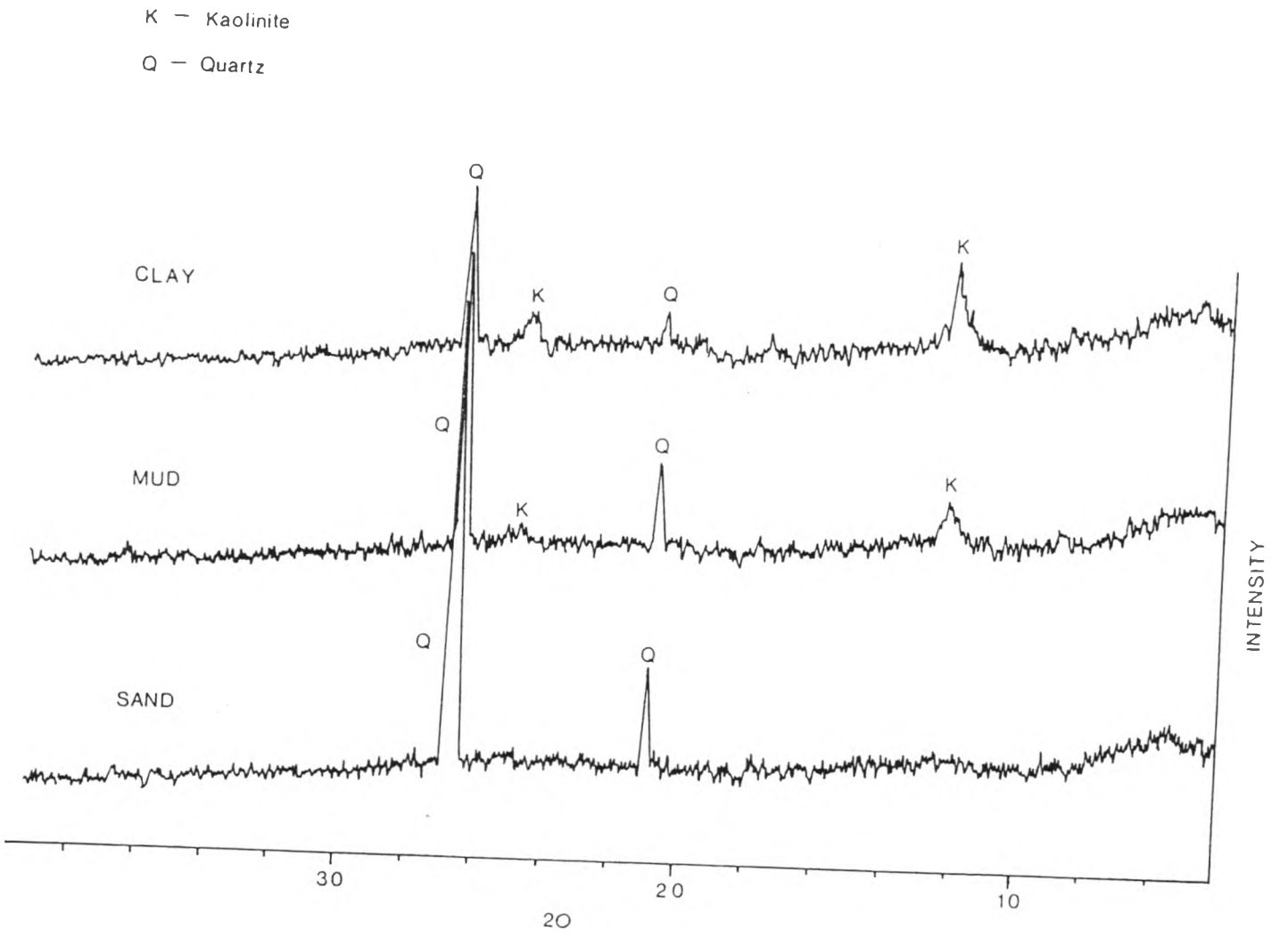

Fig. 4.3 X-ray diffractograms of sand, mud, and clay fractions of claystone from the Mae than basin.

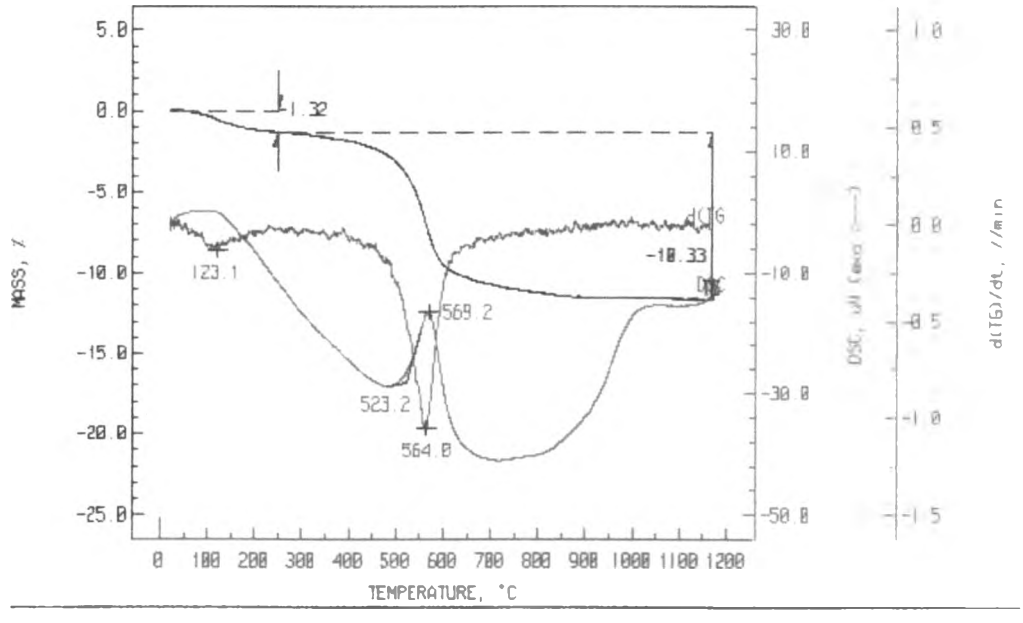

Fig. 4.4 Thermal analyses (blue curve : DTA, red curve : d(TG), and violet curve : TG) of clay sample from drill-hole no. MT-14 at depth between 30-42 metres; heating rate at 10°C/minute under N_2 condition.

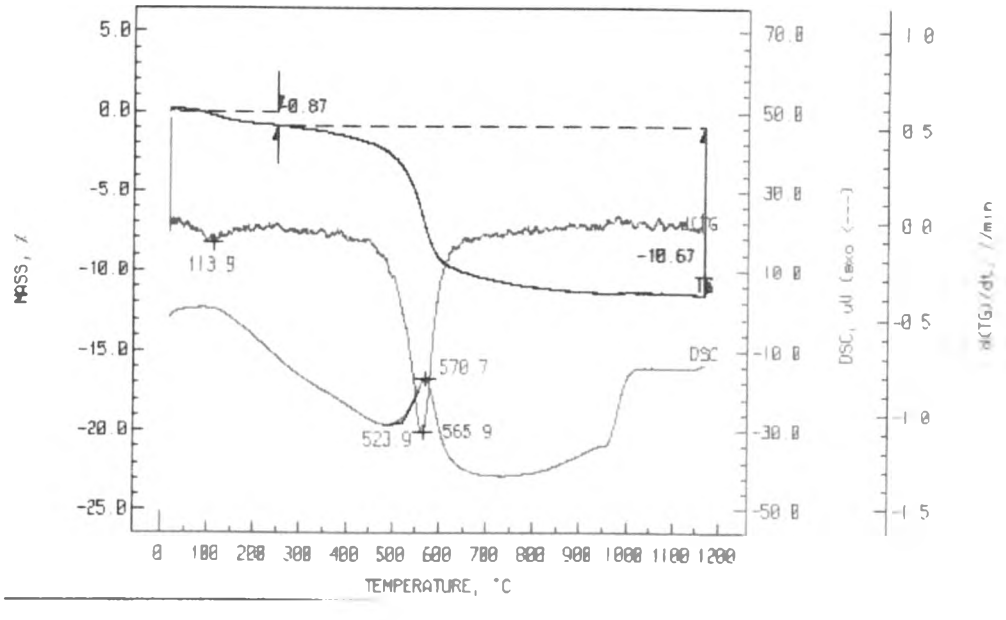

Fig. 4.5 Thermal analyses (blue curve : DTA, red curve : d(TG), and violet curve : TG) of clay sample from drill-hole no. MT-14 at depth between 57-59 metres; heating rate at 10°C/minute under N_2 condition.

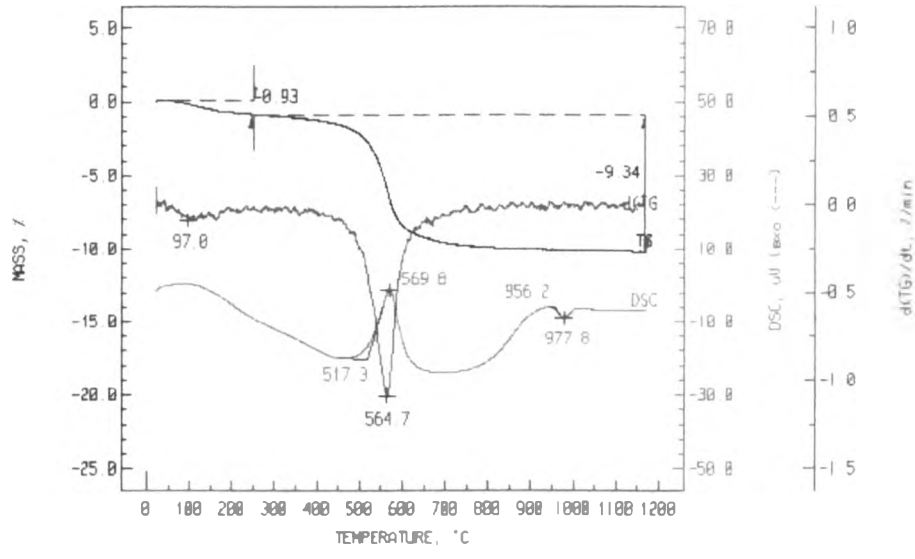

Fig. 4.6 Thermal analyses (blue curve : DTA, red curve : d(TG), and violet curve : TG) of clay sample from drill-hole no. MT-15 at depth between 61.5-69.0 metres; heating rate at 10°C/minute under N_2 condition.

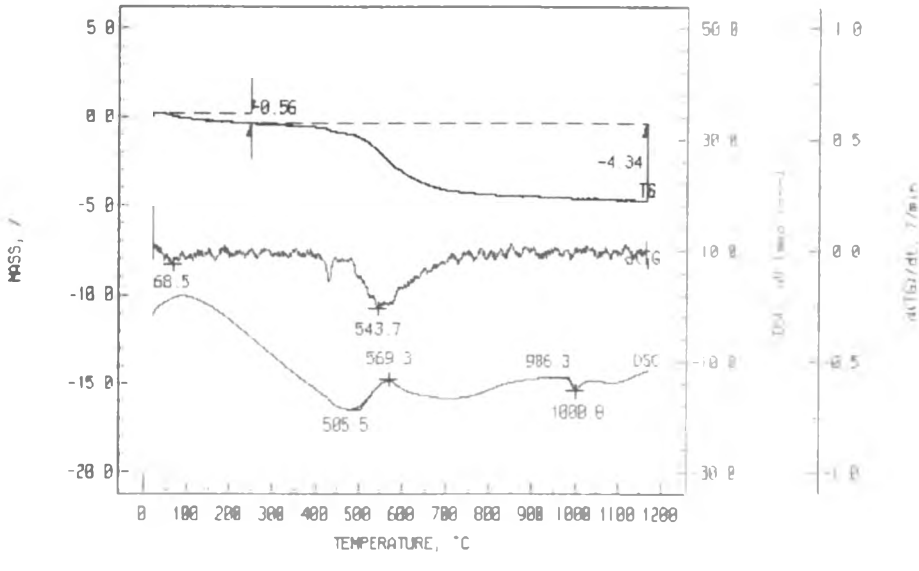

Fig. 4.7 Thermal analyses (blue curve : DTA, red curve : d(TG), and violet curve : TG) of clay sample from drill-hole no. MT-15 at depth between 85-90 metres; heating rate at 10°C/minute under N_2 condition.

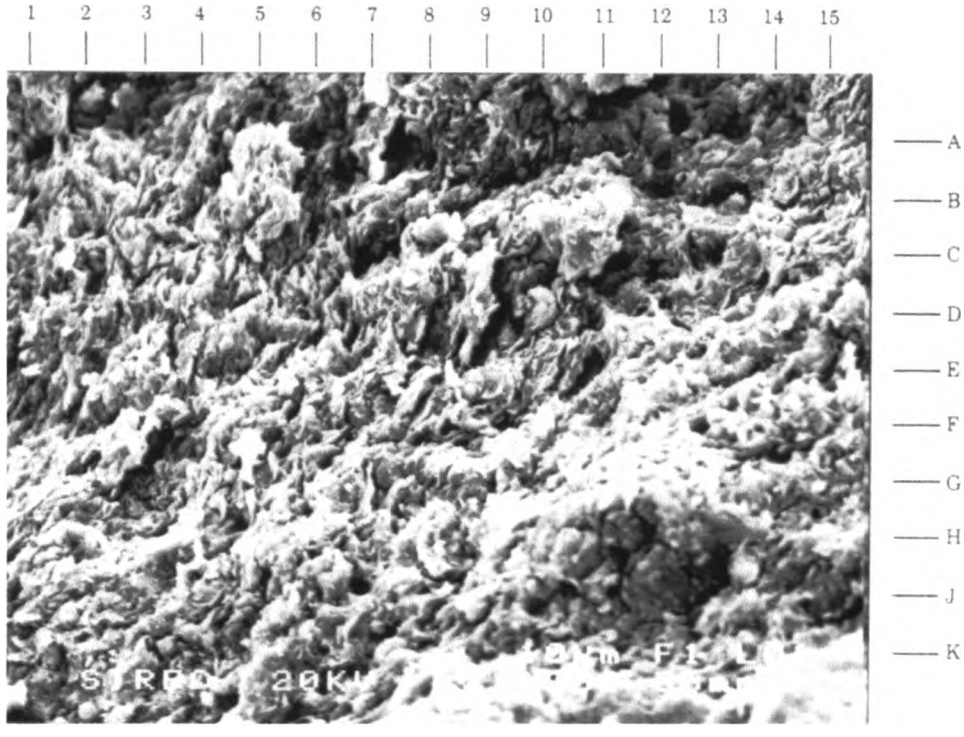

Fig. 4.8 The scanning electron micrograph (SEM) showing an overview of claystone (Unit B) comprising of an aggregate of curved, platy kaolinite and illite.

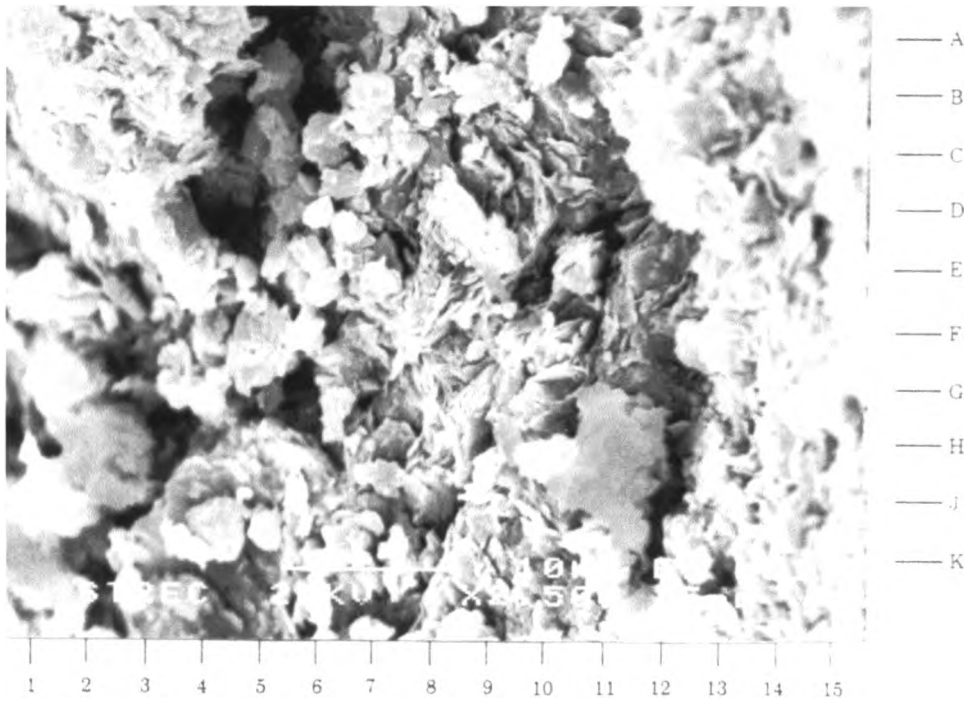

Fig. 4.9 Close up SEM of the Figure 4.8.

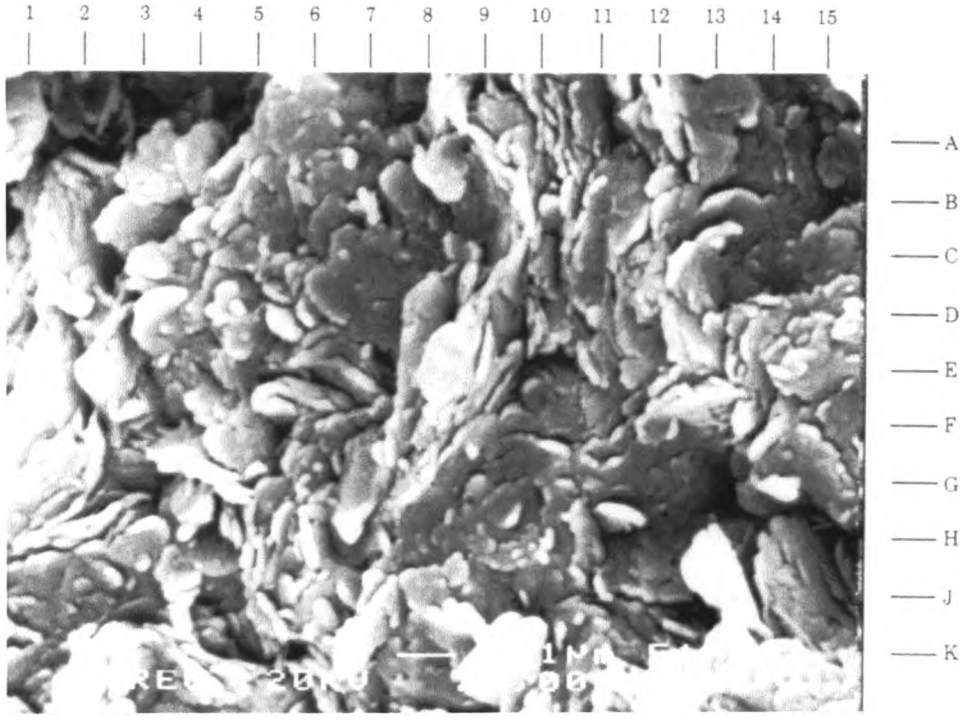

Fig. 4.10 Close up SEM showing the aggregate of curved, platy kaolinite and illite(with EDS data at D8).

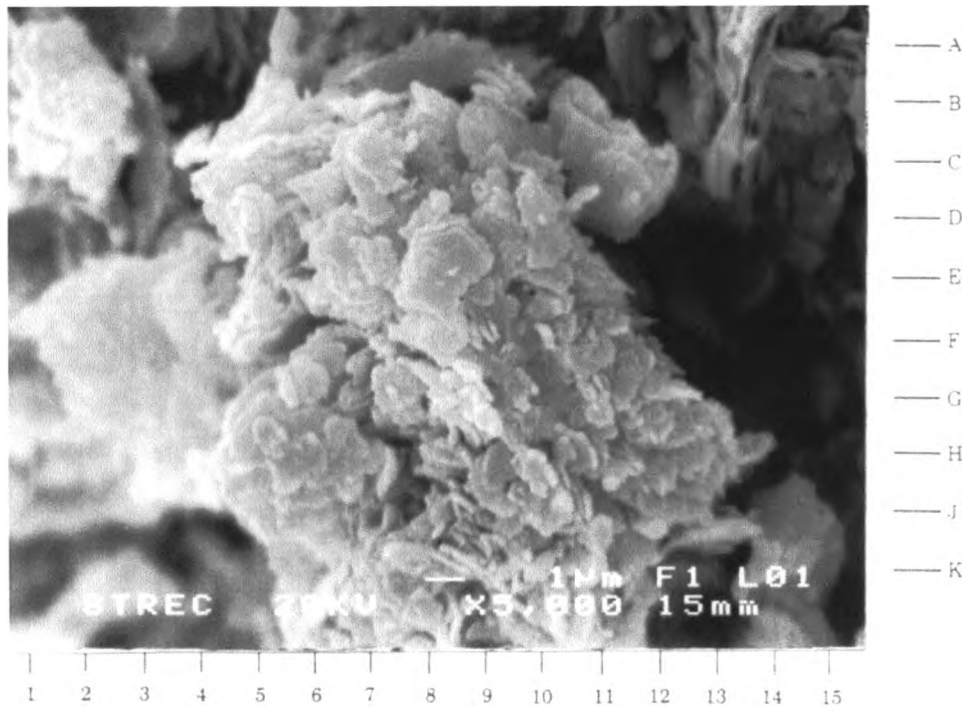

Fig. 4.11 Close up SEM showing the aggregate of irregular border, pseudo-hexagonal kaolinite.

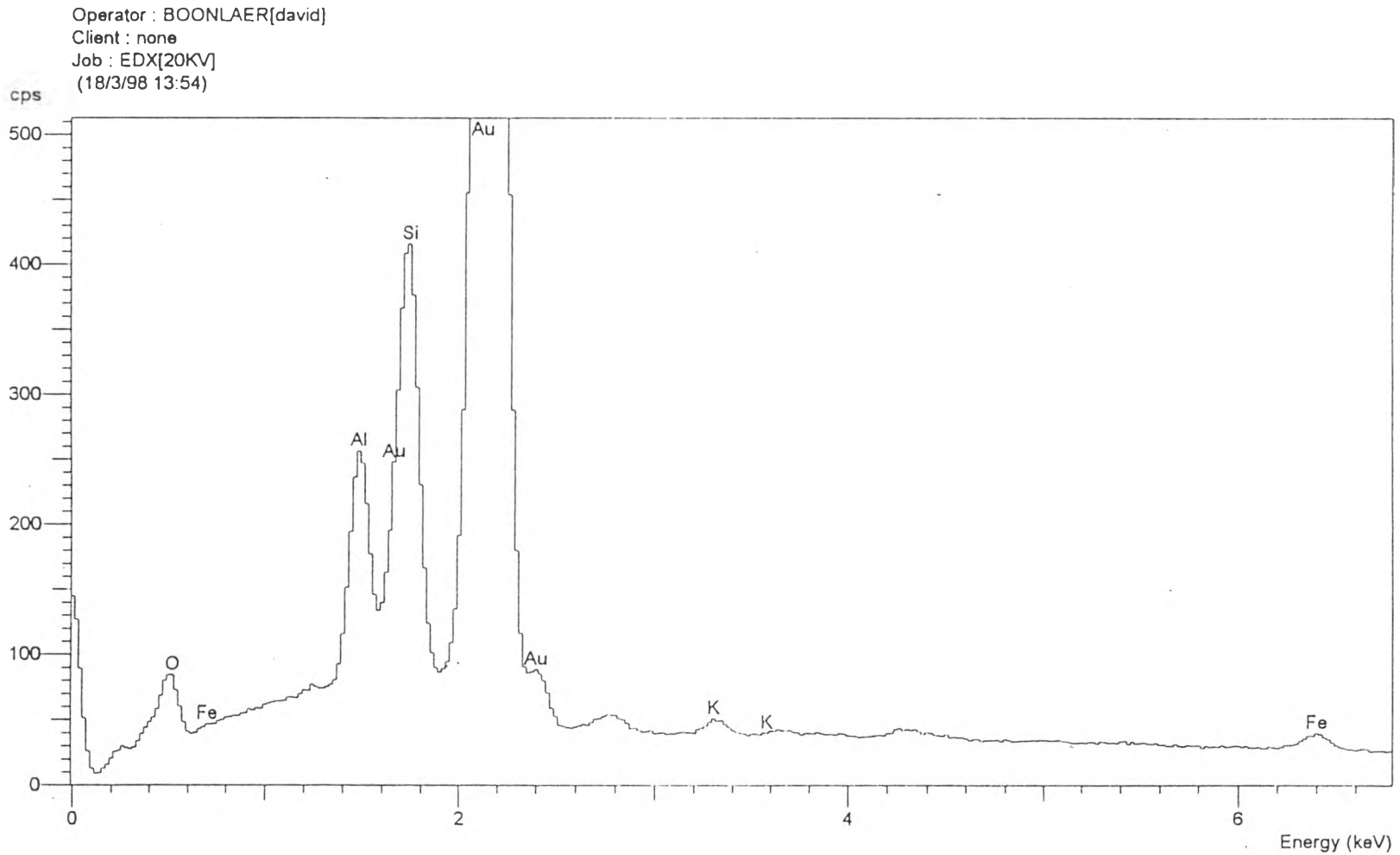

Fig. 4.12 Energy dispersive X-ray spectrum of platy illite.

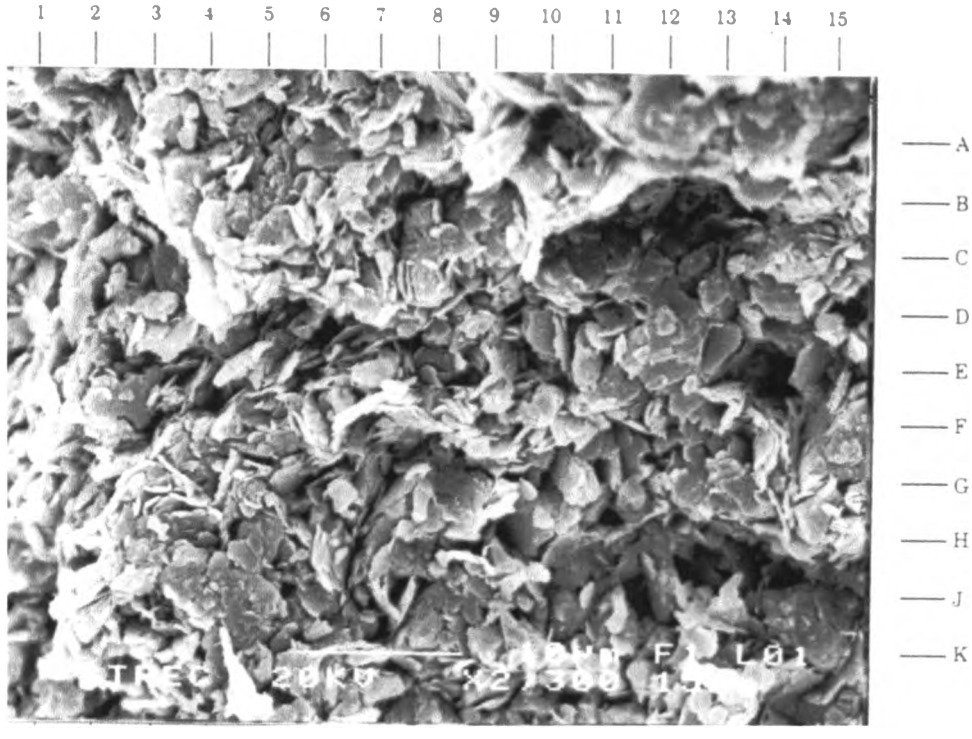

Fig. 4.13 The scanning electron micrograph (SEM) showing an overview of claystone (Unit D) comprising of an aggregate of curved, platy kaolinite and illite.

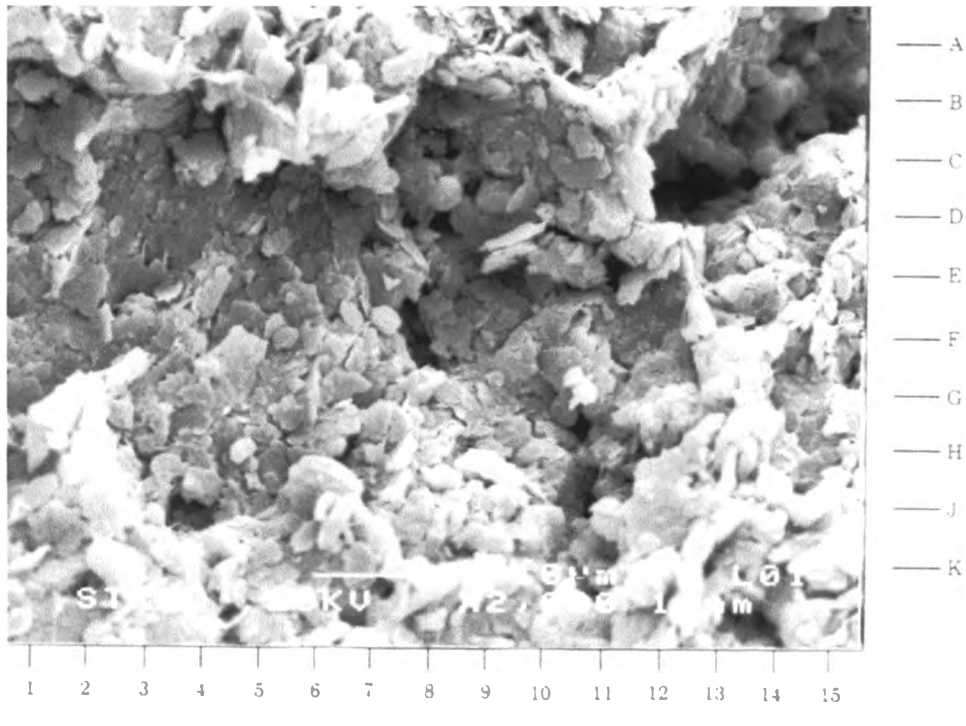

Fig. 4.14 The SEM showing an overview of claystone (Unit D) comprising of the irregular flakes of kaolinite and illite.

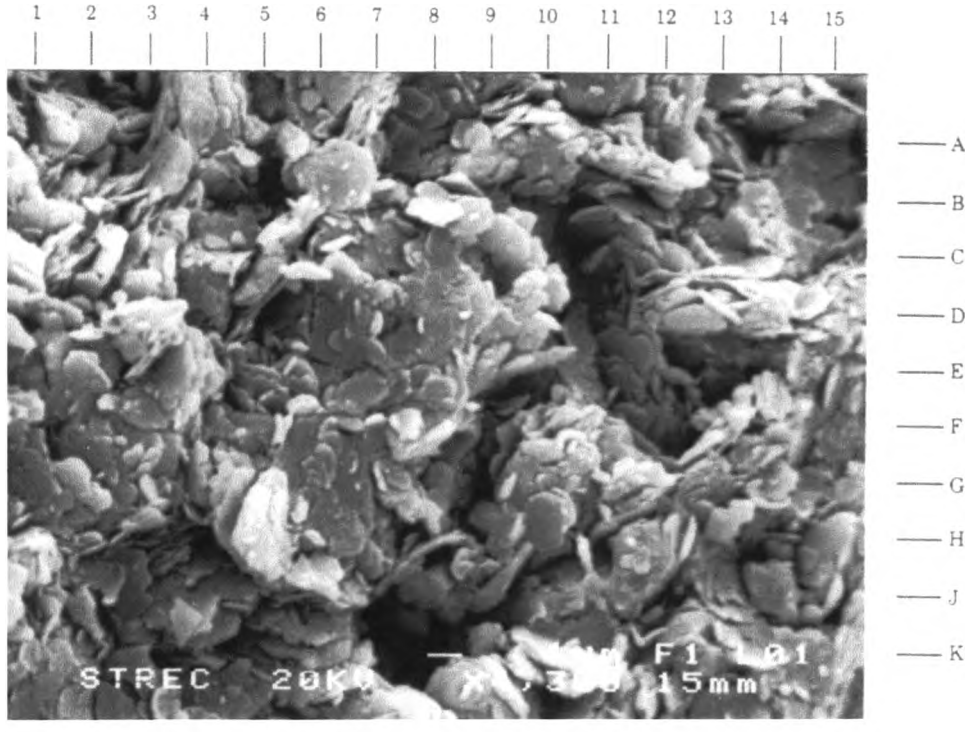

Fig. 4.15 Close up mineral show illite flake with EDS data (D8).

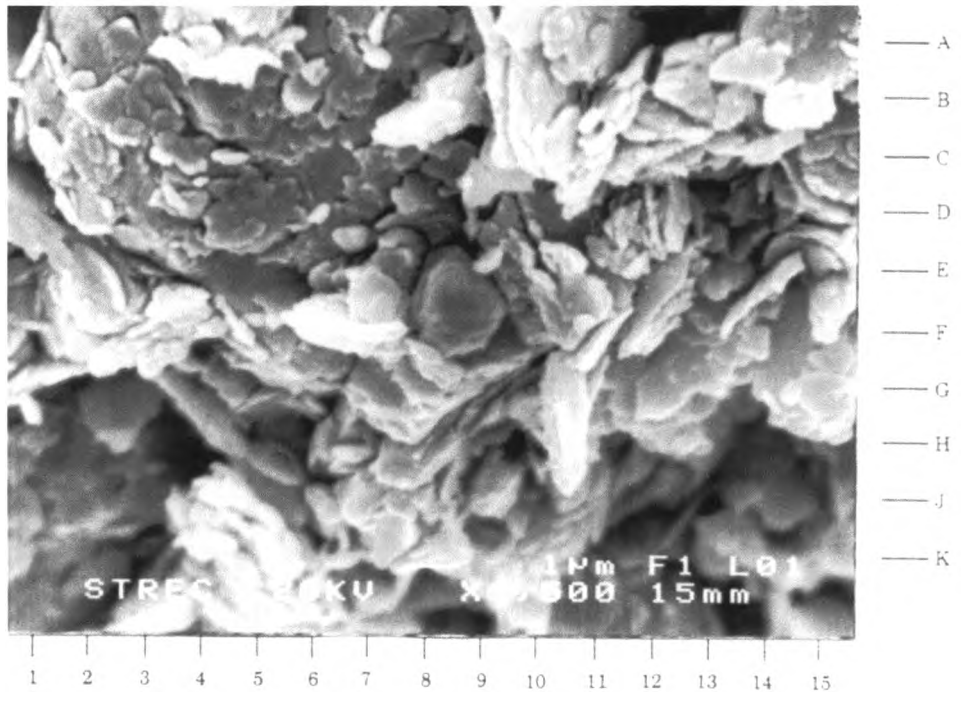

Fig. 4.16 Close up mineral show high sphericity and sub-angular of quartz grain (F8) in claystone between the major two coal seams with EDS data.

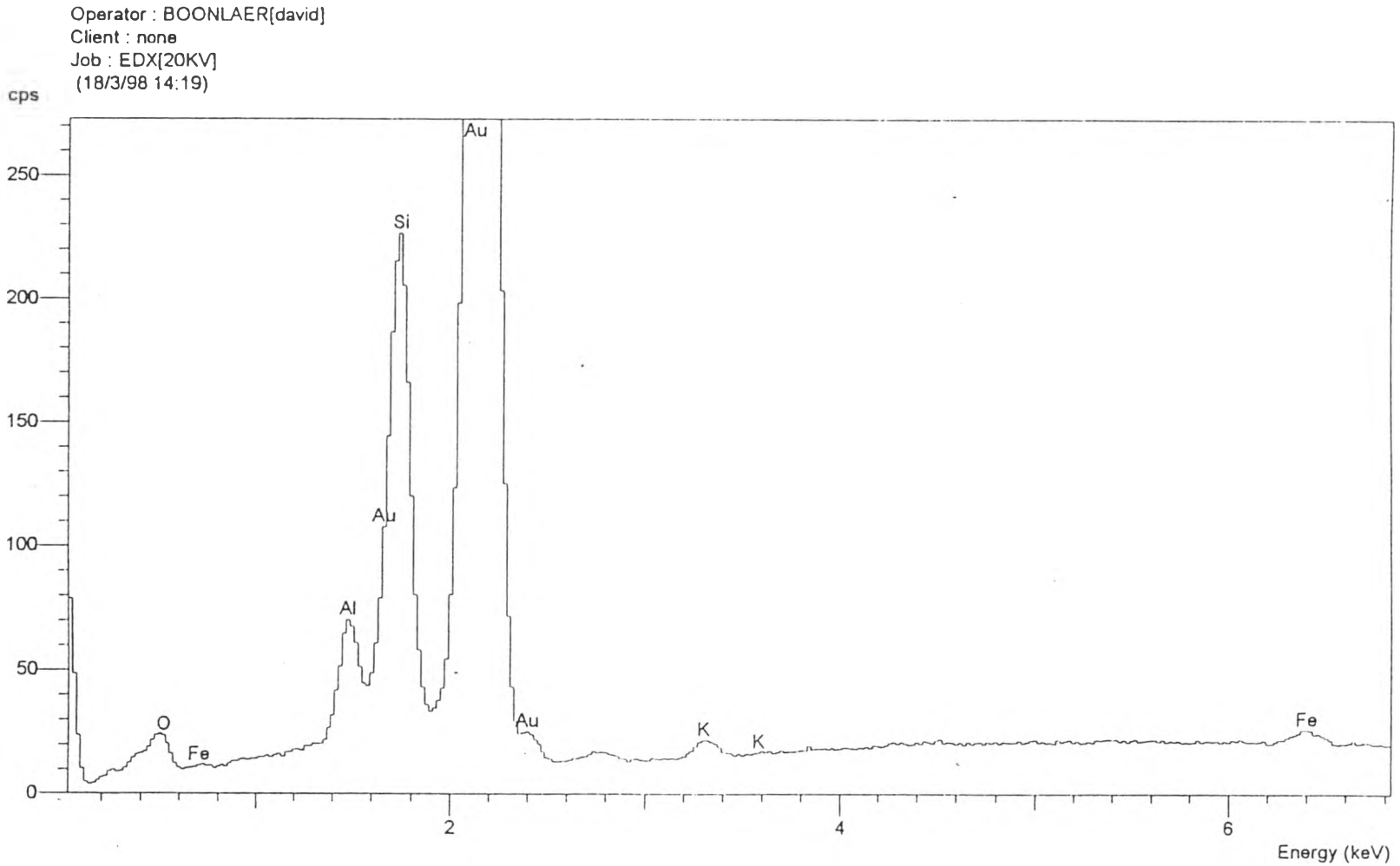

Fig. 4.17 Energy dispersive X-ray spectrum of flaky illite in claystone (Unit D).

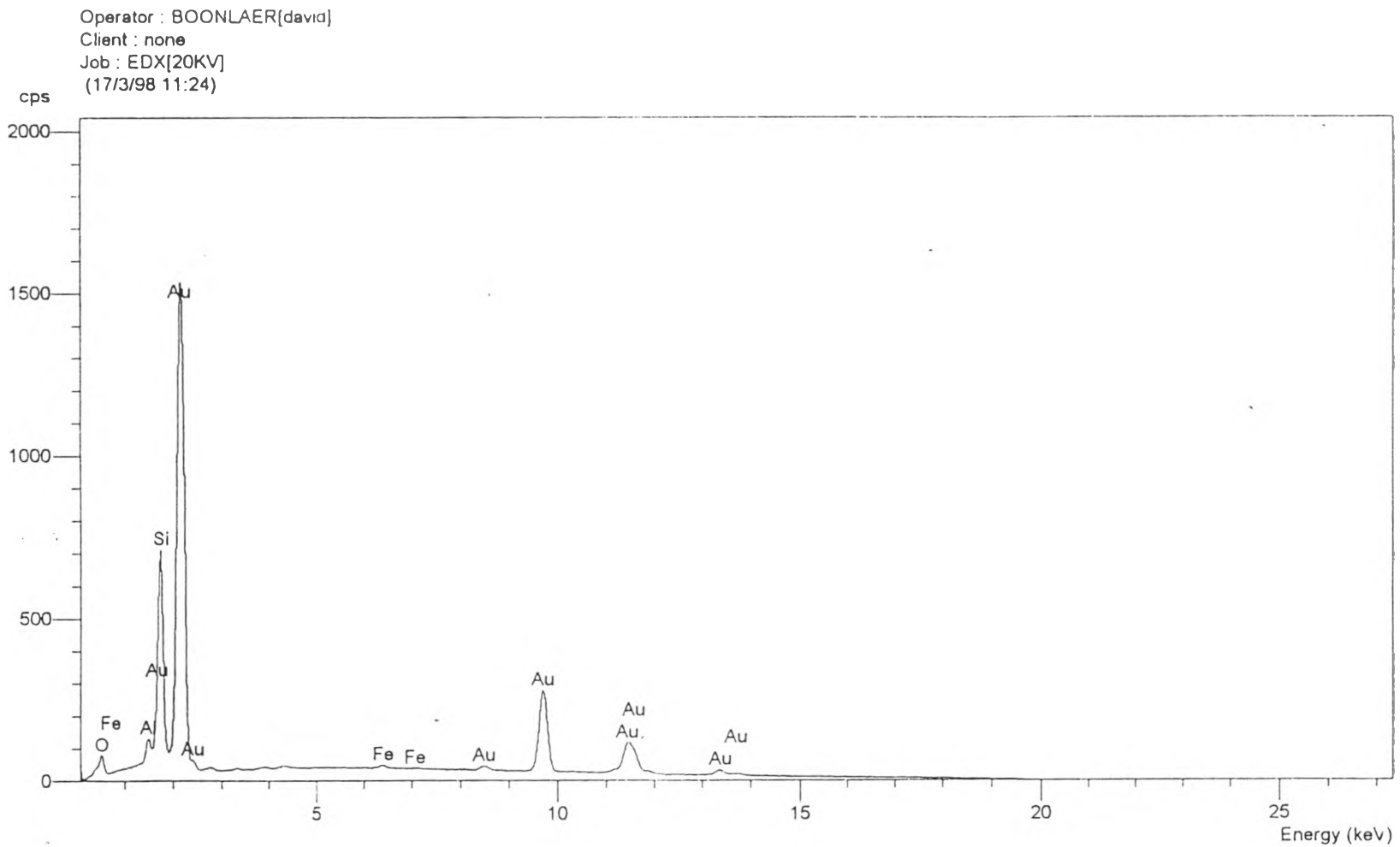

Fig. 4.18 Energy dispersive X-ray spectrum of quartz in claystone (Unit D).

This morphological habit suggest that most of kaolinite and illite are not diagenetic in origin but they are rather derived from erosion and transportation of the pre-Cenozoic source(s). The most likely potential source, as earlier outlined, would be the Permo-Triassic rhyolitic tuff from the western part of the basin. However, minor contribution from the Permo-Triassic volcanics in the north and the Triassic Phra That Formation from the southeastern part of the basin cannot be completely ruled out.

From the detailed study of the mineralogical composition and characteristics of the ball clay from the Cenozoic Mae Than basin earlier described, the following conclusion can be reached

Kaolinite : $Al_2Si_2O_5(OH)_4$

The major clay mineral of the Mae Than claystone is the kaolinite with approximately 34 per cent in content. The crystal habit of kaolinite under the present study as revealed from the electron microscopy shows that it is platy or flaky with broken or irregular crystal outline. This crystal morphology indicates that the kaolinite is of allochthonous origin under the erosion and transportation by the fluid media, or water from the source area as evidenced from the abrasive effects. It is noted that the flaky or platy crystal habit of kaolinite can be differentiate from that of illite by observing the EDS pattern. The kaolinite has the almost equal proportion of silica and aluminum, whereas the illite has the silica exceeding the aluminum. Besides, the EDS pattern of illite exhibits the presence of potassium.

The X-ray diffractograms of almost all samples show that the kaolinite is disordered in characteristics, i.e. broad major peak, slightly shift in the major peak angle. This disordered kaolinite suggests that is was formed under relatively low temperature of weathering process from feldspars of pre-existing felsic rocks (Bristow, 1989). The DTA/TG patterns of kaolinite, with slightly asymmetrical endothermic dehydroxylation peaks (570°C), also indicate that the kaolinite is disordered in characteristic.

It is believed that the kaolinite in the ball clay of the Mae Than basin mainly originated under the intensed chemical weathering and decomposition of plagioclase, K-feldspar, and muscovite, under hot and humid conditions of the pre-existing rhyolitic tuff, exposed in the western margin of the basin. Eventually, the kaolinite was eroded and transported to be deposited under the organic rich fresh-water lake environment in the Mae Than basin.

$$2KAlSi_3O_8 + H_2CO_3 + H_2O \longrightarrow K_2CO_3 + Al_2Si_2O_5(OH)_4 + 4SiO_2$$

orthoclase — carbonic acid — potassium carbonate — kaolinite — silica

Illite : $K_{0-2}Al_4(Si_{8-6}Al_{0-2})O_{20}(OH)_4$

Illite is the second most abundant clay mineral approximately 20 per cent, of the Mae Than ball clay. The electron micrograph of illite is flaky or platy similar to that of kaolinite, but the illite crystal habit does not show the hexagonal outline. The EDS pattern of illite show that the silica content is higher than the aluminum content. Besides, the presence of potassium in the EDS is typically of illite crystal.

The X-ray diffractogram of the Mae Than ball clay show the presence of illite and illite mixed with mixed-layer minerals (illite-smectite) as observed from the peak characteristics. A reasonable mechanism for the formation of illite (Jackson, 1964) entails the partial replacement of muscovite by montmorillonite layers on an atomic scale, giving rise to a higher silica content, partial lattice expandability, and lower potassium content (Berner, 1971). This is in keeping with the idea mentioned earlier that many illites are really mixed-layer mica-montmorillonites.

The illite is formed under the acid weathering conditions with partial leaching of mobile cations, i.e. potassium of feldspar and micas.

$$3KAlSi_3O_8\,(s) + 2H^+\,(aq) \longrightarrow KAl_3Si_3O_{10}(OH)_2\,(s) + 6SiO_2\,(aq) + 2K^+\,(aq)$$

Siderite : $FeCO_3$

The siderite in the ball clay is essentially associated with the lacustrine facies in the form of nodular hard band with spherulitic texture. The X-ray diffractogram definitely indicate the presence of siderite.

The nodules are believed to be formed by diagenetic mobilization of iron under reducing, organic-rich diagenetic conditions of pH 7-8. The mobilization of iron under these conditions is attributed to locally lower pH and soluble organic complexes. The siderite spherulite are a diagenetic products formed by recrystallization of siderite originally disseminated in the argillaceous groundmass.

The ideal conditions for supply of iron to surface waters would appear to be found in tropical, humid areas of low relief and intense chemical weathering. In such, regions complexing of iron with organic acids may increase the delivery of dissolved or colloidal iron to basin of deposition.

Upon exposure to the atmosphere, the siderite spherulite show the reaction rim of iron oxides. This partial oxidation process of siderite has helped to intensify red coloration of nodular hard band and disseminated iron concretions of ball clay both in the mine pit and stock pile.

$$\underset{\text{siderite}}{2FeCO_3} + H_2O \longrightarrow \underset{\text{hematite}}{Fe_2O_3} + 2CO_2 + 2H^+$$